Posted on 21 Nov 2022 — The copyright holder is the author/funder. All rights reserved. No reuse without permission. — https://doi.org/10.1002/essoar.10503609.1 — This a preprint and has not been peer reviewed. Data may be preliminary.

On The Robustness of Asthenosphere Plug Flow in Mantle Convection Models With Plate-Like Behavior

Alana Semple[1] and Adrian Lenardic[1]

[1]Rice University

November 21, 2022

Abstract

The question of what drives tectonic plates has been revitalized by seismic observations that cannot be explained by conventional plate-driving forces. The observations, designed to constrain flow in the asthenosphere, are consistent with the asthenosphere locally flowing faster than the plate above and in a direction offset from plate motion. These inferences are not consistent with plates being driven exclusively by slab-pull and/or ridge-push forces. Mantle convection models were put forth to argue that pressure-driven flow, interacting with a non-Newtonian upper mantle viscosity, could explain these observations. To test the robustness of those results, we expand the models to allow for the development of weak plate margins and associated plate-like behavior. We find that with weak margins, the overall component of slab-driven flow becomes stronger while pressure driven asthenosphere flow remains active. Locally, the asthenosphere can lead plates and there are rotations in the direction of asthenosphere flow with depth. The balance of plate driving forces (i.e., the ratio of slab-pull to asthenosphere flow) is found to depend on plate margin strength. The models also indicate that a non-Newtonian upper mantle allows for a hysteresis effect such that, depending on initial conditions, single-plate and plate-tectonic modes can exist at the same parameter conditions.

On The Robustness of Asthenosphere Plug Flow in Mantle Convection Models With Plate-Like Behavior

Alana Semple[1], **Adrian Lenardic**[1]

[1]Rice University

Key Points:

- Weak plate margins and a power law viscosity asthenosphere allow asthenosphere flow to exceed lithosphere velocity
- There are local regions where asthenosphere flow rotates with depth away from lithosphere flow direction
- Mobile vs stagnant lid state depends on lid strength and initial condition when the asthenosphere has a power law viscosity

Corresponding author: Alana Semple, `ags7@rice.edu`

Abstract

The conventional hypothesis holds that tectonic plates are driven exclusively by slab-pull/ridge-push forces, but this is challenged by recent seismic observations of asthenosphere flow. These observations indicate that the asthenosphere locally flows faster and in a different direction than the plate above. Previous mantle convection models argued that pressure-driven flow with a non-Newtonian upper mantle viscosity can account for these observations. We expand those models by simulating simple plate breaking behavior in plate margins. Under these conditions, the ratio of slab-driven flow to pressure-driven asthenosphere flow increases while pressure driven flow remains active. The ratio of driving forces decreases with increasing plate margin strength. Locally, the asthenosphere can drive plates and change flow direction with depth. Furthermore, a non-Newtonian upper mantle allows for a hysteresis effect where, depending on initial conditions, single-plate (stagnant lid) and plate-tectonic modes can exist at the same parameter conditions.

Plain Language Summary

Conventional wisdom holds that the motion of tectonic plates drives motion in the Earth's rocky interior (i.e., in the Earth's asthenosphere). Recent seismological observations have brought this view into question as they indicate that the velocity of the asthenosphere can exceed tectonic plate velocity. This suggests that interior motions can drive plate motions. We explore models of coupled plate tectonics and interior motions to address this discrepancy. The models reveal that the coupling between plates and the asthenosphere is not an issue of plates drive asthenosphere motion or asthenosphere motion drives plates. Both factors work in tandem with the balance being a function of plate margins strength and asthenosphere rheology. In particular, a power-law viscosity allows pressure gradients to generate interior flow that can locally drive plate motion. The models also reveal a hysteresis effect that allows different tectonic states (plate tectonics versus a single plate planet) to exist at the same parameter conditions. This indicates that history and initial conditions can play a role in determining if a planet will or will not have plate tectonics.

1 Introduction

Since the early days of the plate tectonic revolution, the leading idea for what drives plates has been slab-pull (Cox, 1972; Forsyth & Uyeda, 1975; Schubert et al., 2001; Turcotte & Schubert, 2014). More recent studies have questioned this and argued for a combination of slab-pull and pressure driven asthenosphere flow (Höink et al., 2011; Coltice et al., 2019). Seismic observations from the central Pacific added support to this idea as they could not be accounted for by invoking purely slab-driven flow (Lin et al., 2016). A subsequent study showed that the results were consistent with pressure driven flow interacting with a non-Newtonian upper mantle (Semple & Lendardic, 2018).

The study of Semple and Lendardic (2018) was motivated by seismic observations that showed two distinct shear zones in the asthenosphere and a mis-orientation between asthenosphere and plate flow directions (Lin et al., 2016). The models of Semple and Lendardic (2018) included a power law, upper mantle rheology within a spherical mantle convection model. The power law rheology lead to the formation of a low viscosity channel below a higher viscosity plate analog (i.e., an asthenosphere formed dynamically). Pressure gradients developed in response to upper boundary layer thickening away from zones of upflow (Höink et al., 2011). The low viscosity of the asthenosphere layer allowed it to flow faster than the plate above, in response to the pressure gradient. The pressure driven flow profile flattened toward a plug shape due to the power law rheology. This produced two concentrated shear layers within the asthenosphere (Fig. 1). Spherical geometry allowed pressure gradients to become offset in direction from the direction of upper boundary layer flow generating a change in flow direction with depth (Fig. 1). These findings provided a physical interpretation for the observations of Lin et al. (2016).

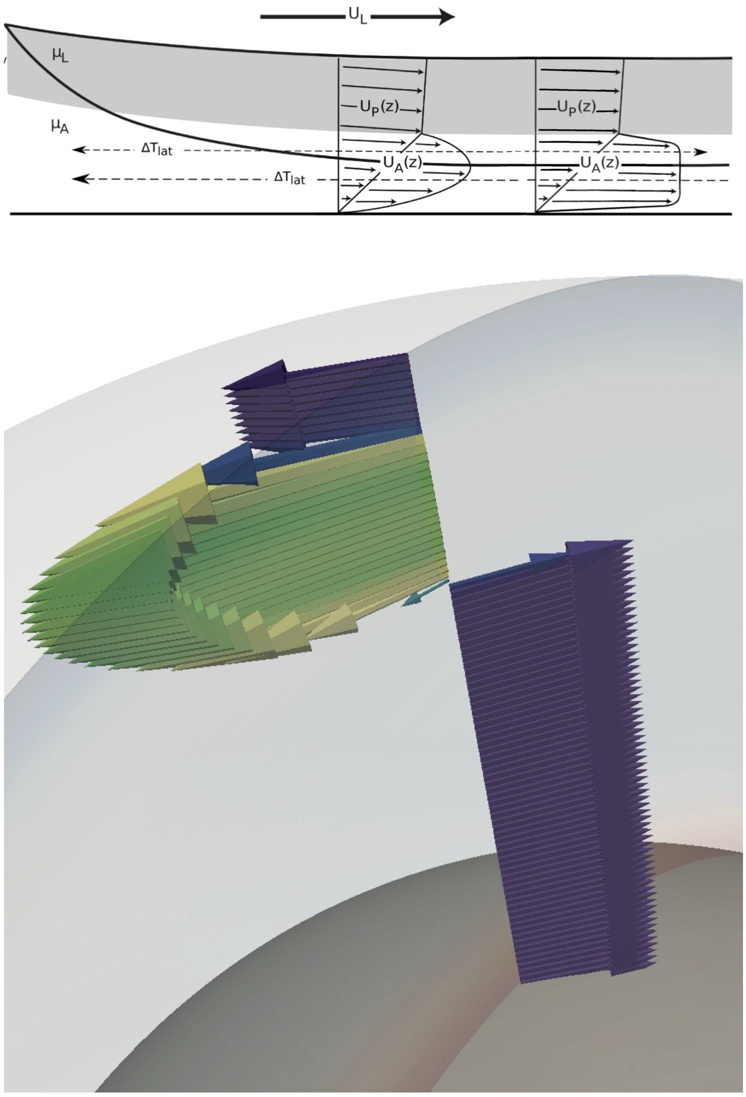

Figure 1. From Semple and Lenardic 2018. Top: Plug flow in the asthenosphere can develop where pressure gradients are strong and non-Newtonian viscosity is applied. Bottom: Newly plotted results from Semple and Lendardic (2018). Perspective view of a velocity profile for their n=3 results. Arrows are velocity vectors colored by viscosity where purple is 1 and greens are very low viscosity. This shows a location with plug flow in the asthenosphere and asthenosphere flow offset from lithosphere direction.

The study of Semple and Lendardic (2018) did not include weak plate margins. Flow in the models was partially driven by the sinking of cold upper boundary layer material into the mantle. This served as an analog for slab driven flow, but it is lacking in the sense that it may underestimate the strength of slab pull. Without weak plate margins, the high viscosity of a plate analog provides resistance to mantle downflow. Allowing for weak plate margins would alter this resistance and could enhance downwelling velocity and, by association, the component of slab driven flow (Bercovici et al., 2000).

The above motivates us to test the degree to which the inclusion of weak plate margins may alter the general conclusions that: 1) Pressure gradients provide a significant driving component for asthenosphere flow; 2) Locally, asthenosphere flow can provide a plate driving force; and 3) Offsets in flow directions between the lithosphere and asthenosphere can occur.

2 Modeling Methods

We used the community finite element code CitcomS to solve the equations for mass, momentum, and energy conservation in a spherical shell (Zhong et al., 2000; Tan et al., 2006; Zhong et al., 2008). We assumed mantle convection was driven by both bottom and internal heating. The bottom heating Rayleigh number and dimensionless internal heat ratio are set to 1e5 and 20 respectively. Both are referenced to the viscosity of the lower mantle. Viscosity was radially stratified to simulate a model lithosphere, model asthenosphere, and model lower mantle. A high reference viscosity (200) was set for the model lithosphere to a non-dimensional depth of 0.95. The asthenosphere reaches to depth of 0.88, and was given a power law rheology with a power law exponent of 2. The lower mantle was set to reference a viscosity of 1 with a Newtonian rheology.

A modified version of CitcomS allows for plate margin formation (Foley & Becker, 2009). When stresses in the model domain exceed a yield stress value, σ_y, viscosity drops. This simulates plate breaking and weak margin formation without needing to resolve deformation along finite faults (Moresi & Solomatov, 1998; Tackley, 1998). We start our models with a strong lid (high yield stress), then lower the yield stress, using the output of the higher yield stress run as the input for the lower yield stress experiment. Once the model transitions from single to multiple plate behavior, we ramp up the plate strength again. We increase the yield stress, beyond the original single-plate value, using the plate-like behavior model as the initial condition. This provides a test to see if non-Newtonian viscosity allows for hysteresis effects akin to those that can occur in models with temperature-dependent viscosity (Weller & Lenardic, 2012; Lenardic et al., 2016).

We will show results from a case where the lid did not yield (stagnant lid) with $\sigma_y = 3.0{*}10^3$, a case with yield generated plate margins and plate-like behavior (mobile lid) with $\sigma_y = 2.8 * 10^3$, and additional cases with $\sigma_y = 3.0 * 10^3$, $4.0 * 10^3$, $5.0 * 10^3$ that maintain mobile lid behavior.

All results were taken after statistical steady state was achieved. Statistical steady state was determined based on Nusselt number and rms velocity time series. Experiments were run with a numerical resolution of 65x65x65 nodes per spherical cap (the full spherical domain was spanned by 12 caps).

3 Results

We visualize isotherms and yielding locations for our model cases in Figure 2. The results are from models with A) strong plate margins ($\sigma_y = 3 * 10^3$) in a stagnant lid state B) a stagnant lid start with weaker plate margins ($\sigma_y = 2.8 * 10^3$) C) a mobile lid start with strong plate margins ($\sigma_y = 3{*}10^3$) and D) a mobile lid start with stronger plate margins ($\sigma_y = 5 * 10^3$). Yellow regions show where the lithosphere is yielding. Hot (red) and cold (blue) isotherms are also plotted. Red isotherms map the central region of mantle upwellings. Blue isotherms map cold sinking lithosphere.

The lithosphere, or 'lid', of Case A in Figure 2 is not yielding. This leads to stagnant lid mode of convection. The cold isotherm, that is prominent in the other cases, remains within lithosphere. There are mantle downwellings, but they occur at higher temperatures than the active lid cases (this is consistent with stagnant lid convection being associated with higher internal mantle temperatures than active lid cases). Multi-

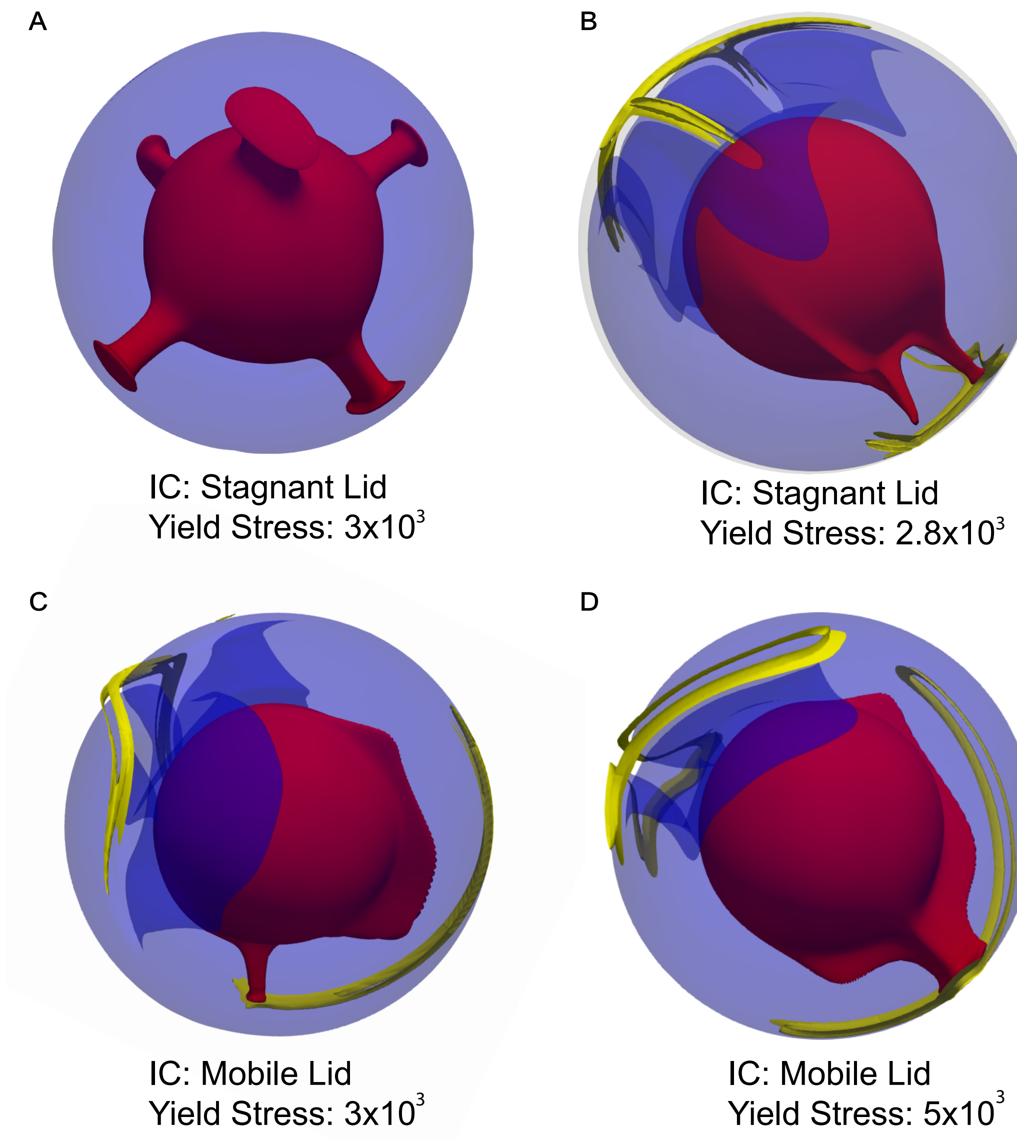

Figure 2. Temperature and yielding visuals from select cases A) initial condition of stagnant lid with a yield stress of $3 * 10^3$ B) initial condition of stagnant lid with a yield stress of $2.8 * 10^3$, C) initial condition of mobile lid with a yield stress of $3 * 10^3$, and D) initial condition of mobile lid with a yield stress of $5 * 10^3$. Colored spheres show isotherms in red (hot) and blue (cold), while yellow regions show where the lithosphere is yielding. Locations where the inner red sphere reach out from the center are upwellings and locations where the blue layer deviates from the outer sphere are downwellings.

ple upwellings signify that this case is associated with relatively short convective wavelengths.

Cases B, C, and D are yielding, indicated by the yellow regions above downwellings and upwellings. All three are in a mobile lid mode of convection. Yielding areas are linear features situated over regions of dominantly vertical mantle motion. The blue isotherms indicate that the lithosphere is "subducting" into the mantle. All three cases tend toward degree-1 convection (i.e., long wavelength flow).

Figure 3 shows radially averaged horizontal velocity profiles with insets showing averaged viscosity profiles over asthenosphere depths (note that the velocities are rms values; velocities change direction, for all the cases, at the asthenosphere-lower mantle boundary). Profiles are for the cases of A) a strong (black) lid, B) a weak (blue) lid, and an increasingly strong lid with a mobile initial condition in C) red, D) teal, and E) brown. Figure 3A reveals an immobile lithosphere. With no lid motion, asthenosphere flow lacks a plate-driven shear component. It develops a parabolic flow profile, indicative of pressure-driven flow, and flows faster than the lithosphere and the lower mantle. The weaker lid and mobile initial condition cases show a fast moving lithosphere, indicating a mobile lid state. As plate margin strength is increased, the lithosphere slows down (Fig. 3B-E). In the mobile lid results, average lithosphere velocity exceeds asthenosphere velocities when lid strength is weaker, but asthenosphere velocities exceed lithosphere velocities as plate margin strength increases. Overall, velocities are increased everywhere in the mobile lid cases when compared to the stagnant lid case. Lower mantle flow reverses direction from upper mantle flow and shows a nearly uniform velocity with depth. Whole mantle convection is maintained for all cases.

Although asthenosphere velocity does not, on average, exceed plate velocity in the weak margin cases, the global velocity profiles indicate that there is still a component of pressure driven flow in the asthenosphere. If the asthenosphere responded passively to plate motion (driven by slab-pull and/or ridge-push), then the velocity profile within it should take the form of Couette flow (shear driven flow with a linearly decreasing flow profile). Our model profiles differ from that expectation (Fig. 3B & C). As plate margin strength is increased, the component of pressure driven flow increases, becoming more prominent in the flow profiles and leading to asthenosphere velocities exceeding lithosphere velocities (Fig. 3E)

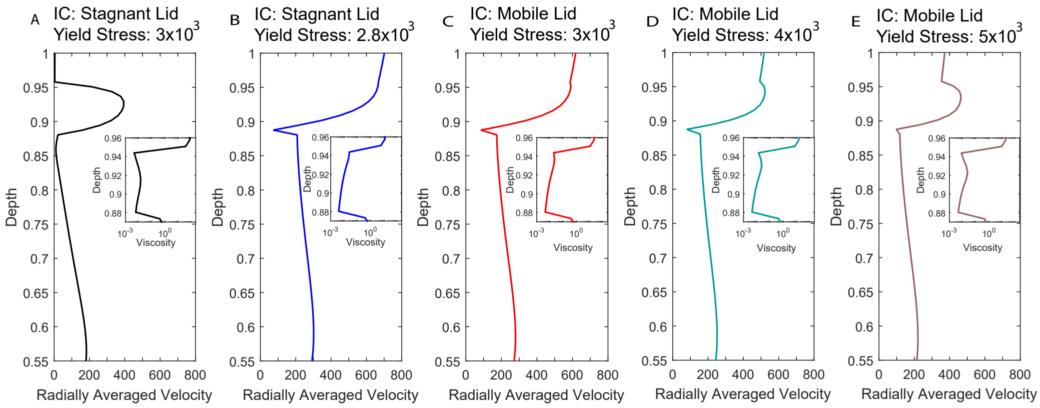

Figure 3. Spherically averaged velocity profiles with inset average viscosity profiles over asthenosphere depths. Profiles are for a A) strong (black) lid, B) weak (blue) lid, and an increasingly strong lid with a mobile initial condition in C) red, D) teal, and E) brown. Velocities are rms values and flow reverses direction from the upper to the lower mantle.

The viscosity of the lithosphere decreases below its reference value where stress is above the designated yield stress. Low viscosity develops dynamically in the asthenosphere owing to a power law viscosity (Fig. 3inset). Viscosity for the stagnant lid case displayed two local minima in the asthenosphere with a maximum in its central region. Weak margin, mobile lid cases had one local minima near the base of the asthenosphere.

As margin strength increased, while maintaining an active lid, a second viscosity minima developed at the lithosphere-asthenosphere boundary (Fig. 3inset). The mobile lid results are associated with cooler interior mantle temperatures than the stagnant lid case and internal temperatures increase with plate margin strength: Average internal mantle temperatures from the cases of Figure 3 are: A) 0.61 B) 0.37 C) 0.39, D) 0.41, E) 0.45.

Local flow profiles can vary from the spherically averaged profiles. Figure 4 presents a view of one such location for two mobile lid cases, A) weak plate margins and B) strong plate margins (from Fig. 2B & D respectively). A perspective view of flow vectors, colored by viscosity, is plotted on the left, with the matching 2D local flow profile on the right. The weak margins case (Fig. 4A) profile was taken near a convergence zone, indicated by the low (yielding) lithosphere viscosity. This profile shows asthenosphere flow (indigo arrows) rotating with depth away from lithosphere direction and to the left (toward the viewer), showing a local region where asthenosphere flow deviates from lithosphere direction with depth. While overall velocities are similar to the global average, the local profile reveals max asthenosphere velocities exceeding lithosphere velocity. This indicates that the ratio of pressure to shear driven flow is larger in this local region than it is on average.

The features discussed above become more pronounced when plate margin strength is increased, while mobile lid convection is maintained. Figure 4B shows asthenosphere flow direction (indigo arrows) offset to the right of lithosphere direction, rotating away from the viewer. In this case, the flow direction offset is prominent throughout all of the asthenosphere, and this offset is also sustained farther away from the convergence zone than in the weakest lid case (Fig. 4A).

4 Discussion

Inclusion of plate-like behavior does not qualitatively alter the principal conclusions of Semple and Lendardic (2018). Quantitatively, the globally averaged profiles of plate-like models show a milder component of pressure-driven asthenosphere flow relative to models that do not allow for weak plate margins. Globally, for weak margins, asthenosphere flow velocities may not exceed plate velocities, but they can do so locally. Within those regions, asthenosphere flow can become offset, with depth, from the direction of lithosphere motion (Fig 4).

In addition to the above, we find a dependence of global plate driving forces on the strength of plate margins (Fig. 3). A stagnant-lid mode results in a large component of pressure driven flow in the asthenosphere. Weak plate margin, mobile-lid behavior leads to a larger component of slab-pull driven flow in combination with a milder component of asthenosphere-drive (Höink et al., 2011). As plate margin strength increases, the component of asthenosphere-drive relative to slab-pull increases. This supports the possibility that plates can be driven by both slab-pull and asthenosphere-drive forces (Höink & Lenardic, 2010; Höink et al., 2011; Coltice et al., 2019).

Our results reveal a hysteresis effect on the value of plate margin strength that allows for mobile-lid convection. This allows different modes to exist under equivalent parameter conditions (2). The potential of hysteresis and bistable tectonics is not a new observations in coupled convection and tectonics models (Weller & Lenardic, 2012). However, those previous models relied on the interaction of temperature-dependent mantle viscosity and dynamic plate margin formation. Our models show that a non-Newtonian upper mantle rheology, together with plate margin formation, also allows for bistabilty. Future models that combine the effects should be considered in order to fully map the range of parameter space that allows for tectonic bistability.

As well as more fully mapping hysteresis effects, there are other expansions to be considered for our experiments. Our power law rheology exponent is below the preferred

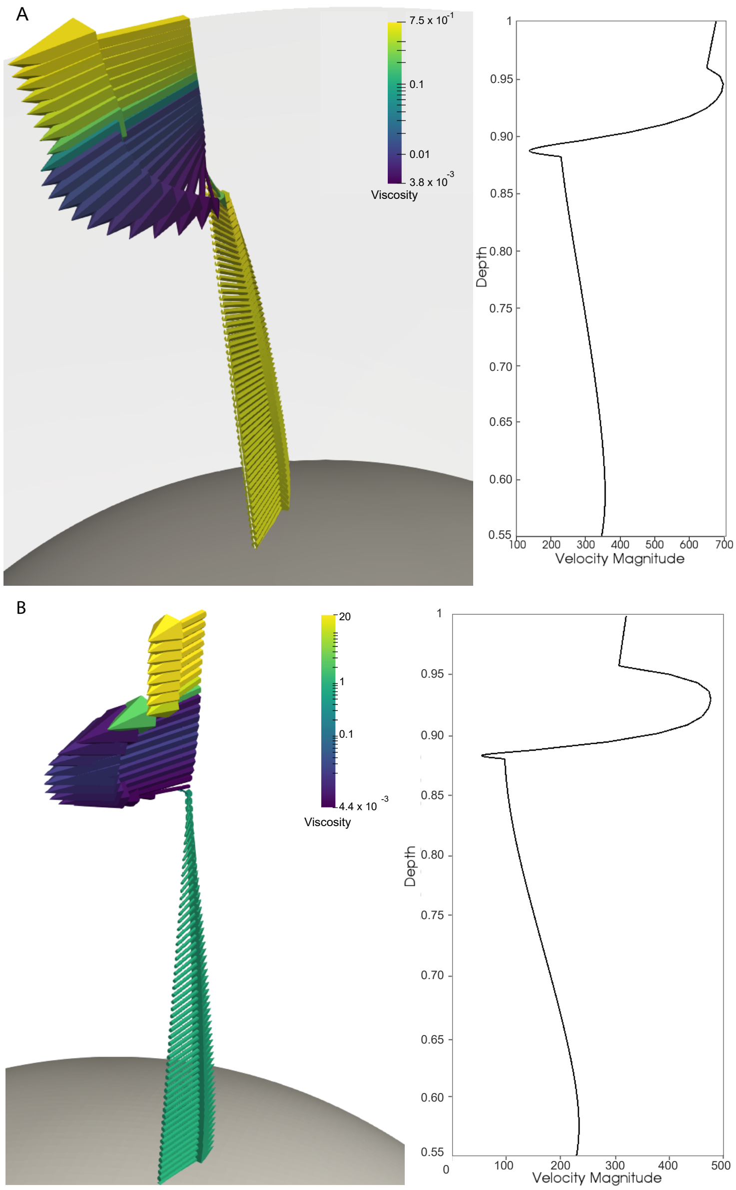

Figure 4. Local velocity profiles for for cases A) $\sigma_y = 2.8 * 10^3$. and B) $\sigma_y = 5 * 10^3$. Left: Perspective view on local profile results where colors indicate viscosity. Right: 2D velocity profile from the matching left image. indigo arrows show asthenosphere depths where asthenosphere flow in both cases rotates away from lithosphere flow and locally leads plate velocities.

rock-like value ($n = 3$) that Semple and Lendardic (2018) tested (Hirth & Kohlstedt, 2013). We kept a lower power law exponent in the interest of keeping the computational burden lower. With non-Newtonian rheology, and yield stress conditions, resolution and run time requirements become large. This is not insurmountable and a sub-goal of our preliminary results was to show that the challenge is worth undertaking (had our new models not confirmed our previous results the motivation to expand them further would be weaker).

5 Conclusions

Allowing for a combination of non-Newtonian asthenosphere rheology and plate-like behavior increases the ratio of slab-pull to asthenosphere-drive forces compared to models that lack weak plate margins (Semple & Lendardic, 2018). None the less, convective flow in the upper mantle remains driven by a combination of slab-pull and pressure-driven flow. In addition, local regions can still exist where 1) asthenosphere velocity exceeds that of the lithosphere above and 2) asthenosphere flow rotates with depth, becoming offset from plate motion.

Acknowledgments

We'd like to our anonymous reviewers for their comments. All input files necessary to run our models and generate this data in CitcomS 3.2 can be found on the online repository, Zenodo, at https://zenodo.org/record/3922867.

References

Bercovici, D., Ricard, Y., & Richards, M. A. (2000). The relation between mantle dynamics and plate tectonics: A primer. *Geophysical Monograph-American Geophysical Union*, *121*, 5-46. doi: 10.1029/GM121p0005

Coltice, N., Husson, L., Faccenna, C., & Arnould, M. (2019). What drives tectonic plates? *Science Advances*, *5(10)*. doi: 10.1126/sciadv.aax4295

Cox, A. (1972). *Plate tectonics and geomagnetic reversals.* W. H. Freeman and Co.

Foley, B. J., & Becker, T. W. (2009). Generation of plate-like behavior and mantle heterogeneity from a spherical, viscoplastic convection model. *Geochemistry, Geophysics, Geosystems*, *10(8)*. doi: 10.1029/2009GC002378

Forsyth, D., & Uyeda, S. (1975). On the relative importance of the driving forces of plate motion. *Geophysical Journal of the Royal Astronomical Society*, *43*, 163-200. doi: 10.1111/j.1365-246X.1975.tb00631.x

Hirth, G., & Kohlstedt, D. (2013). Rheology of the upper mantle and the mantle wedge: A view from the experimentalists. In *Inside the subduction factory* (p. 83-105). American Geophysical Union (AGU). Retrieved from `https://agupubs.onlinelibrary.wiley.com/doi/abs/10.1029/138GM06` doi: 10.1029/138GM06

Höink, T., Jellinek, A. M., & Lenardic, A. (2011). Asthenosphere drive: A wavelength-dependent plate-driving force from viscous coupling at the lithosphere-asthenosphere boundary. *Geochemistry, Geophysics, Geosystems*, *12*. doi: 10.1029/2011GC003698

Höink, T., & Lenardic, A. (2010). Long wavelength convection, poiseuille-couette flow in the low-viscosity asthenosphere and the strength of plate margins. *Geophysical Journal International*, *180*, 23-33. doi: 10.1111/j.1365-246X.2009.04404.x

Lenardic, A., Crowley, J., Jellinek, A., & Weller, M. (2016). The solar system of forking paths: Bifurcations in planetary evolution and the search for life-bearing planets in our galaxy. *Astrobiology*, *16*(7), 551-559. doi: 10.1089/ast.2015.1378

Lin, P. Y. P., Gaherty, J. B., Jin, G., Collins, J. A., Lizarralde, D., Evans, R. L., & Hirth, G. (2016). High-resolution seismic constraints on flow dynamics in the oceanic asthenosphere. *Nature*, *535*, 538-541. doi: 10.1038/nature18012

Moresi, L. N., & Solomatov, V. S. (1998). Mantle convection with a brittle lithosphere: thoughts on the global tectonic styles of the earth and venus. *Geophysical Journal International*, *133(3)*, 669-682. doi: 10.1046/j.1365-246X.1998.00521.x

Schubert, G., Turcotte, D., & Olson, P. (2001). *Mantle convection in the earth and planets.* Cambridge Univ. Press, Cambridge, U. K.

Semple, A. G., & Lendardic, A. (2018). Plug flow in the earth's asthenosphere. *Earth and Planetary Science Letters*, *496*, 29-36. doi: 10.1016/j.epsl.2018.05.030

Tackley, P. J. (1998). Self-consistent generation of tectonic plates in three-dimensional mantle convection. *Earth and Planetary Science Letters*, *157(1)*, 9-22. doi: 10.1016/S0012-821X(98)00029-6

Tan, E., Choi, E., Thoutireddy, P., Gurnis, M., & Aivazis, M. (2006). Geoframework: Coupling multiple models of mantle convection within a computational framework. *Geochemistry, Geophysics, Geosystems*, *7*, Q06001. doi: 10.1029/2005GC001155

Turcotte, D. L., & Schubert, G. (2014). *Geodynamics*. Cambridge Univ. Press, Cambridge, U. K.

Weller, M. B., & Lenardic, A. (2012). Hysteresis in mantle convection: Plate tectonics systems. *Geophysical Research Letters*, *39(10)*. doi: 10.1029/2012GL051232

Zhong, S., McNamara, A., Tan, E., Moresi, L., & Gurnis, M. (2008). A benchmark study on mantle convection in a 3-d spherical shell using citcoms. *Geochemistry, Geophysics, Geosystems*, *9*, Q10017. doi: 10.1029/2008GC002048

Zhong, S., Zuber, M. T., Moresi, L., & Gurnis, M. (2000). Role of temperature-dependent viscosity and surface plates in spherical shell models of mantle convection. *Journal of Geophysical Research*, *105(B5)*, 11063-11082. doi: 10.1029/2000JB900003